Transp Porous Med (2016) 112:749–763
DOI 10.1007/s11242-016-0675-1

Measurement of Relative Humidity to Monitor Salt Migration in Unsaturated Porous Media

R. Hird[1] · **M. D. Bolton**[1]

Received: 24 August 2015 / Accepted: 7 March 2016 / Published online: 18 March 2016

Abstract When aqueous sodium chloride evaporates, crystals can form. Salt crystallisation can take place within voids resulting in subflorescence which can culminate in surface heave, or can lead to efflorescence on exposed surfaces. Evaporation can be measured using relative humidity sensors, and thus salt crystallisation be inferred. A series of laboratory experiments were conducted using vertical flow columns packed with dry medium-grained sand with their exposed surfaces subjected to air at low relative humidity while stood in a shallow container of deionised water or brine. Experiments using deionised water showed that the degree of saturation above the capillary fringe was initially insufficient for transporting salt to the surface through diffusion. Nevertheless, repeated tests using concentrated sodium chloride solution showed that internal changes in relative humidity, and surface heave, were consistent with the upward migration of salt by autogenous internal 'wicking'. The results indicate that relative humidity sensors can be used as a practical way to detect salt crystallisation and the conditions which promote its transportation.

Keywords Salt migration · Relative humidity · Autogenous wicking · Heave

1 Introduction

The movement of salt in unsaturated granular media is poorly understood. In studies of desert soils, which are largely unsaturated, salt is considered to move as a result of climatic or anthropogenic changes to water tables, enabling the capillary rise of saline groundwater (Stokes et al. 2012). It will be shown, however, that salt crystallisation can extend above a saline reservoir, travelling up non-porous surfaces through a wicking mechanism, first described as 'creep' by Washburn (1926) and later by Hazlehurst et al. (1935). The process begins with evaporation causing the brine solution to become supersaturated, followed by

---

✉ R. Hird
rh500@cam.ac.uk

[1] Geotechnical and Environmental Group, Department of Engineering, University of Cambridge, Trumpington Street, Cambridge CB2 1PZ, UK

the nucleation of crystals at the brine meniscus. Further crystals then develop from the solute films that bound the crystals (Desarnaud and Shahidzadeh-Bonn 2011; Dopfer et al. 2013) releasing water vapour (Mullin 2001; Van Enckevort and Los 2013) and the process is repeated, leading to the formation of a dendrite of crystallisation. This creates a fine-grained microporous medium which enhances the upward movement of solute by capillary action, thus advancing the crystallizing front in the fashion of a wick. If autogenous wicking can equally occur inside a porous material, it would supplement capillary rise through the initial pore structure, enhancing the ability of salt to migrate upwards through a column of dry sand above the water table. Unchecked, this could lead to unexpected subflorescence and efflorescence which are significant causes of damage in the fields of soil science, building science and heritage conservation. If salt wicking does take place within dry porous media, then it should be detectable by measuring changes in the internal relative humidity.

Previous studies of porous media, saturated by imbibition with aqueous sodium chloride, have largely focussed on the effect it has on drying kinetics (Or et al. 2013; Norouzi Rad et al. 2015). The role of salt efflorescence has also been studied with regard to the transportation of solute and how this can control the evaporation rate (Eloukabi et al. 2013). Sghaier and Prat (2009) found that efflorescence could initially increase the evaporation potential by wicking of solute through porous salt crystals but only if hydraulic connectivity is maintained. Within indurated granular media, research has focussed on structural deterioration due to salt crystallisation achieved through the wetting and drying processes with water-soluble salts including sodium chloride (e.g. Rodriguez-Navarro and Doehne 1999). In some cases, references to internal relative humidity have been made to understand the stability of water-soluble minerals and computer models have been used to simulate internal relative humidity changes (e.g. Castellazzi et al. 2013).

Changes in evaporation rate can be associated with primary and secondary crystallisation (Desarnaud et al. 2015) and during development of subflorescence Sghaier et al. (2014).

Controlling relative humidity to promote internal solute transport and crystallisation in porous media is widely practised. However, this is often carried out on the exterior of the material being studied and the expected internal changes in relative humidity are inferred. An example is the identification of salt weathering in porous stone which requires either the measurement of external conditions of ambient relative humidity or the destructive removal of samples to check for salt contamination (e.g. Colston et al. 2001; Sandrolini and Franzoni 2006). Furthermore in experimental studies, rates of evaporation from porous media containing solute tend to be estimated by weight loss of water. Relative humidity sensors could easily be embedded within porous media to check conditions which promote salt transportation and be used as a remote monitoring system.

Aside from agricultural studies, documented evidence describing the use of relative humidity sensors to directly or indirectly monitor changes in porous media are rare. Mohamad et al. (2000) measured relative humidity changes to determine solute dispersion through fine granular media and Likos and Lu (2003) devised a practical method to infer suction in fine-grained soils. More research is therefore required to demonstrate the benefits of in situ relative humidity measurement in porous media.

A series of experiments have been performed using vertical flow columns packed with dry sand, and standing in a container of brine, in order to investigate the salt transport mechanism above the saturated capillary fringe. This paper explores the use of buried relative humidity sensors to indicate the presence of salt. To check whether salt migration was occurring through autogenous wicking in dry soil, or by fluid transport within interconnected pore spaces in the saturated capillary fringe, the fluid distribution was first examined using deionised water as the wetting medium. Experiments were conducted at constant temperature, with a static

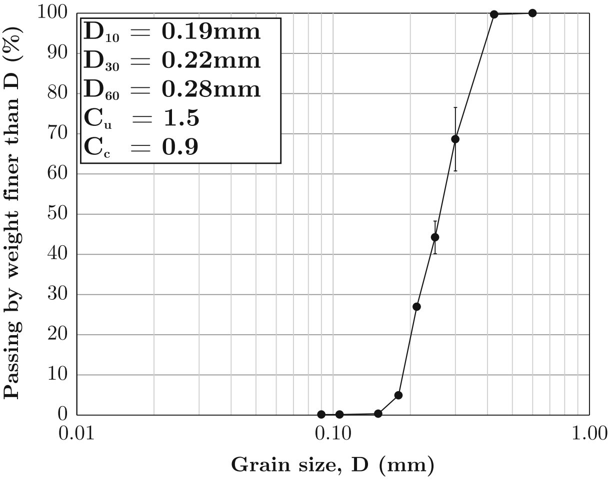

Fig. 1 Grading curve for Fraction D sand

groundwater level and with a low relative humidity airstream at the surface to promote evaporation flux.

2 Method and Materials

2.1 Solute

The groundwater saline concentration was 350 g of sodium chloride reagent (Sigma Aldrich$^{\mathrm{TM}}$ $\geq$ 99.8 % purity) dissolved into one litre of deionised water. This relates to 5.98 moles NaCl per one litre of water where 6.2 moles is the concentration at saturation.

2.2 Granular Medium

The granular medium used in the flow column experiments was a subrounded, natural silica sand supplied by the David Ball Group (Cambridge, UK). The grading curve in Fig. 1 shows that Fraction D is a well sorted or poorly graded sand as defined by the relationships between the coefficient of uniformity (C_{u}) and the coefficient of curvature (C_{c}). The sand was washed and air-dried prior to use.

The particle size range chosen was found to retain a saturated capillary fringe height of 105 mm at 20 °C and should sustain a saturated capillary fringe height of about 102mm for water and 63 mm for 6 M sodium chloride brine at 35 °C, as explained below. This estimate was based upon an equivalent capillary tube using the Young–Laplace equation:

$$h_{\mathrm{c}} = \frac{2T.\mathrm{Cos}\theta}{\rho_{\mathrm{w}}.g.r} \tag{1}$$

where h_{c} is the capillary height, T is the surface tension, θ is the equilibrium or static contact angle between substrate and fluid, ρ_{w} is the density of the fluid, g is the acceleration due to gravity and r is the equivalent pore radius. This equivalent radius was estimated by separate capillary rise experiments in the same sand but with pure water.

Water content measurements in separate columns of Fraction D sand, which had been allowed to achieve a stable capillary rise of pure water at 20°C, were obtained by weighing soil slices taken at 30 mm intervals at the end of the experiment. The saturated capillary height of pure water was thereby estimated to be 105 mm (±15 mm). This corresponds to an equivalent pore diameter in equation 1 of between 0.25 and 0.33 mm. The effective pore diameter of soil is often assumed to be the diameter of particles representing the 10 % fine fraction (or D_{10}) (Terzaghi and Peck 1964). The D_{10} value for Fraction D sand based upon sieve analysis (shown in Fig. 1) is approximately 0.19 mm, which is seen to slightly underpredict the Young-Laplace pore diameter in this case.

To estimate the capillary height of pure water at 35°C, the value for surface tension has been taken as 70.41 mN/m (Vargaftik et al. 1983) and density of 0.994 g/cm^3 (Tanaka et al. 2001). Culligan et al. (2005) reported a contact angle of water in dry silica sand as high as 58° noting that this challenged the usual assumption of wettability. Without published values at 35 °C, a contact of 0° has been considered which will, in any case, overestimate the capillary height. Using equation 1, the capillary height of water at 35 °C is estimated as 102 mm (± 15 mm).

The justification of values used to transform the capillary height from water to brine are based upon published data and independent tests of surface tension and contact angle. Sadeghi et al. (2010) measured the surface tension of brine at sodium chloride concentrations up to 3M and at temperatures between 30 and 60 °C and showed a reduction of 0.2 mN/m per 1 °C. These values matched independent checks of surface tension using 5 M sodium chloride at 25 and 30 °C. Ozdemir et al. (2009) measured the surface tension of 6M brine as 81 mN/m at 20 °C and so a value of 78 mN/m should be appropriate at 35 °C.

Sghaier et al. (2006) measured the static contact angle of aqueous sodium chloride at 20 °C and at various concentrations by the sessile drop method on chemically cleaned glass microscope slides. Independent tests to measure the dynamic contact angle at 25, 30 and 35 °C in 5M sodium chloride solution were carried out on chemically cleaned glass plate using the Wilhemy balance method. The Wilhemy balance is an indirect force measurement of the effects of fluid on a vertically inserted glass plate. As the plate remains in contact with the fluid at constant concentration, this allows better temperature control than the sessile drop method. At an insertion rate of 0.1 mm/s to a depth of 5 mm, no temperature effects were found on the advancing contact angle. This would suggest that the static contact angle of 50°, extrapolated from the data presented by Sghaier et al. (2006), for 6 M aqueous sodium chloride could also be applied at 35 °C. Laboratory analysis with a 5 M solution of sodium chloride between 25 and 35 °C showed the density of aqueous sodium chloride to reduce by 0.01 g/cm^3 over a 15 °C increment. A value of 1.182 g/cm^3 has been taken as the density of 6 M sodium chloride at 35 °C. Using these values, the estimated height of the saturated capillary zone of brine in Fraction D sand, in the absence of evaporative internal salt crystallization, is 63 mm ± 10 mm.

2.3 Relative Humidity Sensors

Combined relative humidity (RH) and temperature chips were used in the flow column experiments to measure the conditions inside the soil above the estimated height of the saturated capillary fringe. The sensors were manufactured by Sensirion© (Switzerland) of type SHT71 which have an accuracy of ± 3 % RH between 20 and 80 °C and overall dimension of 20 × 5 × 3 mm. The chips sensing element (6 ×4 mm) comprises a capacitive sensor for measuring relative humidity and a band-gap sensor for temperature measurement, both coupled to a 14 bit analogue to digital converter. Each sensor is supplied pre-calibrated by the manufacturer with calibration coefficients programmed into the memory on the chip. This reduces the need for re-calibration. For measurements in soil, the exposed circuits on the chip were protected against potential water immersion using silicone conforming cement to the recommendations of the manufacturer but leaving the 2.1 × 0.4 mm cavity on the sensing chip exposed. The sensors were connected to an evaluation kit (EK-H4) made by Sensirion© which included a four-channel multiplexer and logger. The connection between the sensors' 4 pin legs and the cable to the multiplexer was also sealed using silicone cement protected by heat shrink. Trial tests close to the surface of 6 M brine and placed within a stream of water mist gave relative humidity measurements of 74 and 100 % respectively, as they should.

2.4 Time Domain Reflectometer

The presence of polarising fluids within the sand was sensed using time domain reflectometry (TDR) with three-rod probes. TDR is a common method for measuring changes in dielectric constant utilising the technique of electromagnetic wave propagation through solid metal rods acting as wave guides. The waves travel to the end of the waveguide and are reflected back. The additional delay before the electromagnetic wave returns depends upon the dielectric contrast at the end of the wave guide, and this is sampled in TDR measurement. A Campbell Scientific® TDR100 (Logan, Utah, USA) was used in the flow column experiments, which combines a fast time pulse generator with a pulse length of 14 µs and a timed response (pulse generator and sampling circuit) of less than 300 ps. The system allows the user to select the waveform sampling resolution, which depends on the cable length and average velocity along with the length of conductor to be sampled and the signal resolution, soil properties and length of the probes. The TDR100 is connected to a multiplexer (SDMX50), also supplied by Campbell Scientific®, allowing up to eight separate measurements.

Three-rod probes of 50 mm length, 1.44 mm diameter and composed of 316 grade stainless steel were fabricated in-house according to the method described by Robinson et al. 2003. The probes were then calibrated to measure the offset caused by differences in dielectric constant between the coaxial cable and the junction of the probes. An empirical relationship between dielectric constant and volumetric water constant was obtained by inserting the probes horizontally into Fraction D sand which was then compacted to a porosity of 0.4 and saturated with deionised water before being allowed to drain naturally.

2.5 Proximity Sensor

To measure changes in the surface height at the top of the column, without contact to the surface which might alter water vapour and salt movement, a laser proximity sensor (Baumer OADM 12I6430/S35A) with a 10 mm maximum sensing range was used. Readings were made using a National Instruments™ logging unit.

2.6 Flow Column

The flow columns used in the experiments were 300 mm high × 100 mm internal diameter × 5 mm wall thickness and composed of transparent cast acrylic. A 50 mm long × 140 mm OD section of acrylic tube referred to as the 'top cap' was mounted on a stainless steel flange of the same outer diameter and an internal diameter of 100 mm. The flange was attached to the flow column by placing screws through the column walls. A clear acrylic disc of 140 mm outer diameter was attached to the top of the top cap with an air diffuser placed at the centre—the diffuser would allow low humidity air to be distributed evenly at the top of the

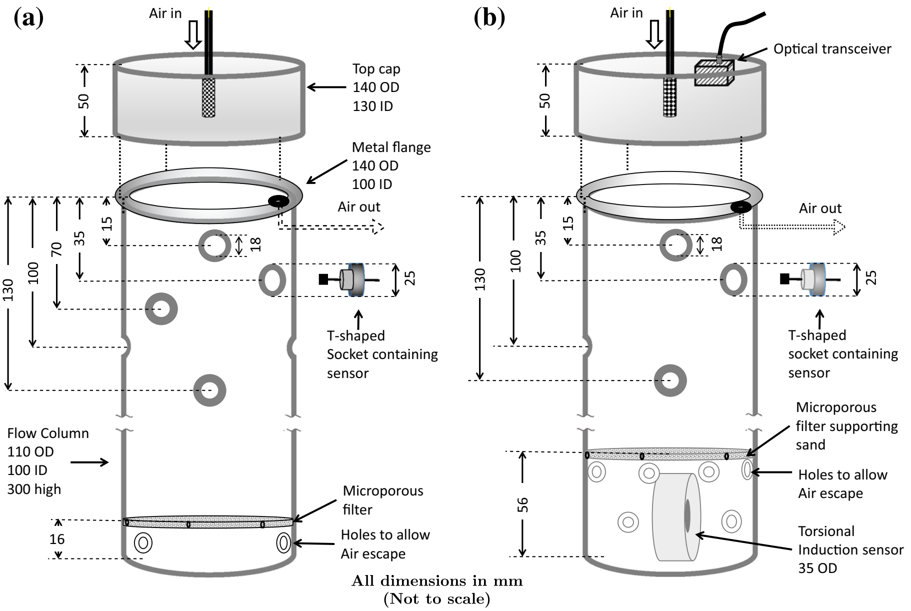

Fig. 2 Flow columns setup. **a** For deionised groundwater, **b** for NaCl brine groundwater

column. An outlet for air was placed at the base of the top cap. A plastic 105 μm microporous filter (SPC Technologies Ltd, UK) of 4 mm thickness and 100 mm outer diameter was placed above the base, inside the flow column, by wall mounted supports. Holes drilled into the walls at and below the filter allowed air to escape when the column was stood in a container of water or solute acting as the groundwater. Sensors were sealed into 'T'-shaped sockets so that they could be mounted at the side of the column and be embedded in the sand. Holes to accommodate the sockets were cut through the flow column walls and were 18 mm in diameter with a 25-mm countersink on the outside of the column to fit the sockets and ensure a good seal. Sensor positions were chosen so that they were located above the estimated top of the saturated capillary fringe to measure changes in the unsaturated part of the column.

The height of the filter (and thus the base of the sand) in the flow column was adjusted so the saturated capillary fringe height of both water and brine would be approximately the same. The layout of the flow column for capillary rise experiments is presented in Fig. 2a for deionised water and Fig. 2b for 6 M brine. For the experiment with deionised water as the groundwater, dual sensors comprising relative humidity chips and TDR probes sensors were placed into the wall of the flow column at depths of 15, 35, 70, 100 and 130 mm below the top of the column (see Fig. 3a). For the experiment using brine as the groundwater, relative humidity sensors were placed at 35, 100 and 130 mm depth (see Fig. 3b). A further sensor was placed at 15 mm depth in some of the tests. An actual instrumented column test is shown in Fig. 3c.

The setup of both columns was the same. Sand was added in layers with the column on a vibratory table so that the sensors were completely embedded, and to ensure an even packing. Two tests were carried out using deionised water, and four using 6 M brine. Differences in packing density for each experiment are presented in Table 1. The top cap was attached to the top of the column, and low humidity air was allowed to flow over the top surface of the sand at a rate of 10 L/min and exit just below the top cap. The columns were then placed in

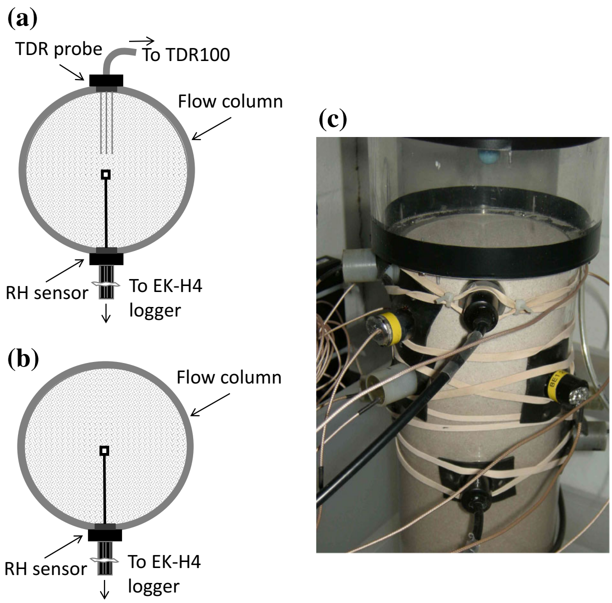

Fig. 3 Plan view of sensor orientation in column used with deionised water (**a**) and 6M NaCl brine (**b**); instrumented flow column under test (**c**)

Table 1 Properties of each test for deionised water and brine as the wetting medium

Groundwater medium	Deionised water		6M NaCl brine			
Experiment	(A)	(B)	1	2	3	4
Dry density (g/cm^3)	1.68	1.68	1.7	1.68	1.68	1.71
Porosity (−)	0.37	0.37	0.36	0.37	0.37	0.35
Air flow relative humidity (%)	10	1	1	1	1	1
Groundwater level (mm)[a]	270	270	220	225	228	232
Estimated capillary height (mm)[a]	168	168	157	162	165	169
Monitoring period (h)	300	300	97	278	326	83

[a] Below top of column

a shallow container of either deionised water or 6M brine acting as groundwater, and placed in an incubator kept at constant 35 °C (± 0.5 °C) temperature. To prevent the groundwater from evaporating, a thin layer of olive oil was placed between the outside wall of the flow column and the exposed groundwater in the container. The groundwater level was maintained in each case using a peristaltic pump connected to a tank containing the same fluid at the beginning of the experiment. The groundwater level for the experiments with water was kept the same, but for those with brine groundwater the level was slightly changed to increase the unsaturated zone above the saturated capillary fringe. As an added precaution, a torsional induction sensor was placed beneath the base of the sand in the brine groundwater to monitor the concentration of the solute by means of electrical conductivity.

3 Results and Discussion

The upward movement of water into dry sand is governed by adhesive and cohesive molecular forces creating surface tension. Air in the pores is displaced by water rising through the soil to create a capillary fringe. The top of the capillary fringe marks the point where the interfacial forces acting between air–water and water–solid interfaces are in equilibrium with the weight of fluid in the saturated zone below. However, any tendency for evaporation may influence the geometry of the capillary fringe, and especially the unsaturated vadose zone above it; Yang et al. (2004) therefore suggest that standard values may best be achieved by covering the column surface to prevent evaporation. This would, however, create a top boundary condition unrepresentative of the conditions that promote efflorescence, which was the practical focus of this investigation. In this experiment, the surface was not covered and instead air of low relative humidity was allowed to pass over the surface.

3.1 Experiments Using Deionised Water at the Base

How the relative humidity of the airstream influences the distribution of water above the capillary fringe was first examined in the two experiments where deionised water had been maintained to a level 30 mm above the base of the column. Figure 4 presents the change in dielectric constant (measured using TDR) at time intervals 24, 98, 135 and 300 h for experiment (A) which was exposed to 10 % relative humidity at the surface and experiment (B) where 1 % relative humidity at the surface was maintained. In both experiments, dielectric constant is shown to increase downwards towards the estimated level of the saturated capillary fringe. The natural range of mineral soil lies between a relative permittivity of 2 and 5 and values above this must contain water. Figure 4 shows that the change in relative humidity at the surface appears to have an effect on the dielectric constant above the capillary fringe. To convert dielectric constant to fluid saturation, it is necessary to first determine the volumetric water content relationship (which is unique to each probe) and take into account the sample porosity. Figure 5 presents the same data as in Fig. 4 but converted to degree of saturation. At a sensor elevation of 130 mm, the saturation is 0.6 where the relative humidity is at 10 % at the surface, compared to 0.3 where relative humidity at the surface is 1 %.

The internal distribution of relative humidity within the soil above the capillary fringe can be measured using the soil-embedded relative humidity sensors. Figure 6 presents the change in relative humidity at each of five sensor elevations beneath the surface. The data are shown using a 10 % relative humidity air stream at the surface. It can be seen that the relative humidity rapidly increases up to around 98 h before reaching an equilibrium state. At this point, the relative humidity remains close to 98 % for the duration of the experiment. The sensor cannot operate when immersed in water so it is known that fluid does not reach the lowest sensor elevation. At 70 mm below the surface of the column, the relative humidity remains at 96 % but reduces towards the surface.

The significantly lower relative humidity shown by sensors at 35 and 15 mm below the top of the column is influenced by the incoming air flow. The water vapour in the sand column diffuses upwards according to the humidity gradient and is then removed at the surface by the airflow.

Knowing the effect on saturation as a result of changing the relative humidity of the air stream at the surface, the distribution of fluid in the pore space can now be examined. This will

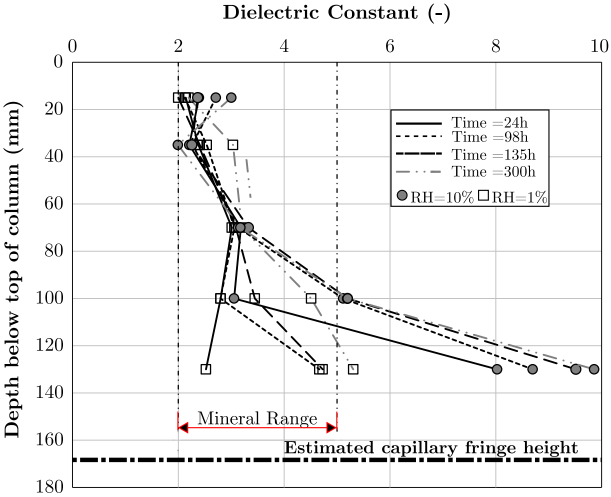

Fig. 4 Evolution of dielectric constant above deionised groundwater at each sensor elevation in relation to a surface relative humidity of 10 and 1 %

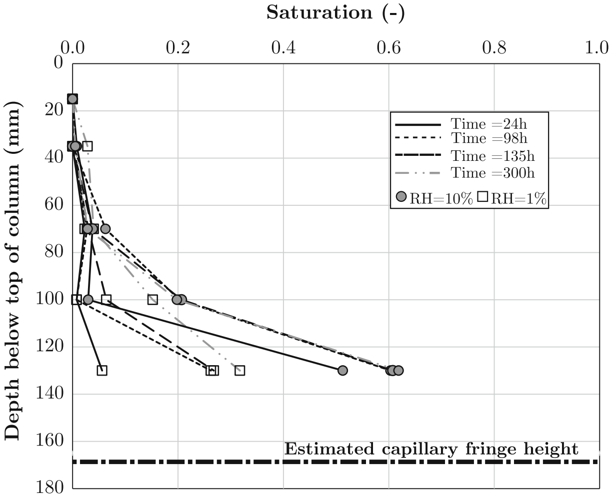

Fig. 5 Evolution of saturation above deionised groundwater at each sensor elevation in relation to a surface relative humidity of 10 and 1 %

establish whether salt dissolved within the groundwater could reach the surface of column by diffusion.

By combining the data from Figs. 5 and 6 for experiment (A), the relationship between fluid saturation and relative humidity can be established. Figure 7 presents the fluid saturation distribution versus relative humidity above the capillary fringe. Limits have been added at 0.95 and 0.15 saturation which were suggested by Robert and Soga (2010) to mark different moisture regimes in sand with a similar grading: zone III which is saturated except for possible air bubbles; zone II with a funicular regime of water intercalated with air; and zone I with isolated fluid droplets. A cartoon added at the top of the figure depicts the possible fluid

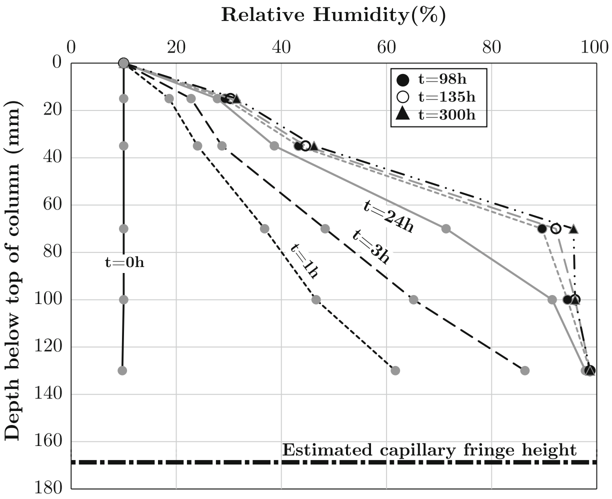

Fig. 6 Evolution of relative humidity above deionised groundwater at each sensor elevation in relation to a surface relative humidity of 10 %

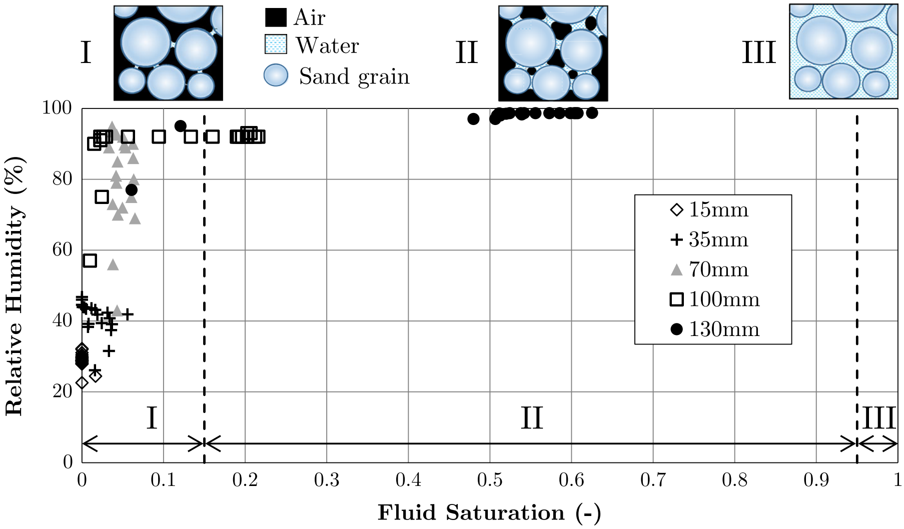

Fig. 7 Variation of saturation with relative humidity above a saturated capillary fringe in the presence of 10 % surface relative humidity. Marker labels refer to sensor depth below the top of the flow column

distribution for each zone. The saturation drops below 0.1, and the relative humidity falls below 50 %, for the higher sensors within 35mm of the top of the column.

Fluid held in funicular formation between soil pores would retain the capacity to transport salts by diffusion, but isolated pendular droplets of fluid would not. Reduction of relative humidity at the surface to 1 % would reduce the internal fluid distribution further. The flow column experiments have thus shown that using low relative humidity air at the surface of the column of sand precludes the possibility of interconnecting fluid existing far above the capillary fringe.

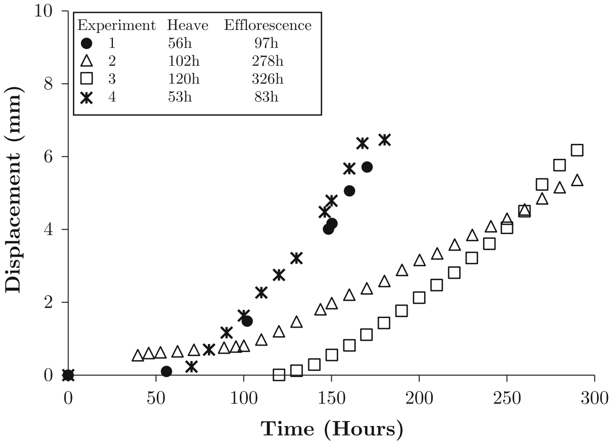

Fig. 8 Surface heave

3.2 Experiments Using 6 M Brine at the Base

Figure 8 presents the surface movement (heave) resulting from subflorescence, for each of the four experiments where brine is used as groundwater. A stream of 1 % relative humidity air at 10 L/min was maintained at the surface. The differences between experiments can be attributed to the formation of salt dendrites which arise through a percolation process which is inherently heterogeneous (Hird and Bolton 2014, 2016). Salt efflorescence was recorded by visual observation. The point when salt heave begins and the later visual observation of salt at the surface provide convenient time markers to analyse changes in internal relative humidity. These time markers are referenced in Fig. 8.

The variation in relative humidity over the course of up to 300 h, measured at each sensor elevation of 130, 100 and 35 mm below the top of the flow column, is presented for each experiment in Figs. 9, 10, 11 and 12. Relative humidity at 15mm below the top of the column was measured in two experiments only because the socket was used for other sensors associated with a wider investigation of salt migration (see Hird and Bolton 2016).

Relative humidity above an aqueous sodium chloride solution is lower than that above water. When sodium chloride crystals can steal sufficient water vapour and return to an aqueous phase, the relative humidity of the surrounding air is referred to as the deliquescent relative humidity (DRH) which varies between 74 and 77 % (Langlet et al. 2013). The relative humidity at the point of salt crystal desiccation is referred to as the efflorescent relative humidity (ERH) which ranges between 41 and 56 % depending on the salt particle size (Gao et al. 2007). These approximate boundaries have been placed on Figs. 9, 10, 11 and 12; between them, salt crystals can coexist with the humid air. Markers representing the start of salt heave and efflorescence have also been shown on the figures as (H) and (E), respectively. The data show that the relative humidity closest to the capillary fringe lies between the ERH and DRH and only in elevations closer to the top of the column do they show higher relative humidity. In experiments 2 and 3, where the relative humidity sensor lies at 15 mm depth, there is a gradual increase in relative humidity above that sensor, notwithstanding the nearly dry air stream maintained across the sand surface. It is expected that the same phenomenon also occurs in experiments 1 and 4 which show a similar relative humidity increase in the sensor at 35 mm depth, but at earlier times. The rise of relative humidity close to the surface

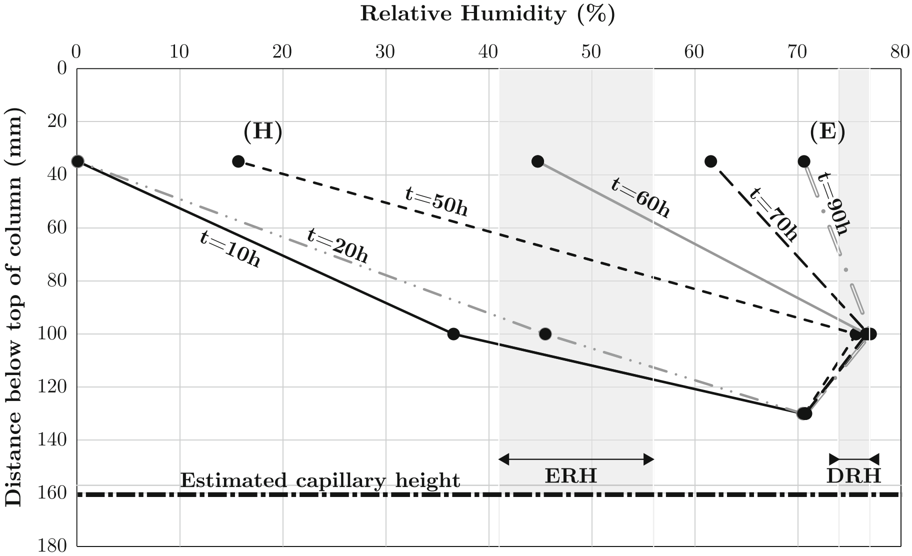

Fig. 9 Relative humidity distribution and evolution according to sensor elevation for experiment 1 showing approximate time of heave (H) and efflorescence (E)

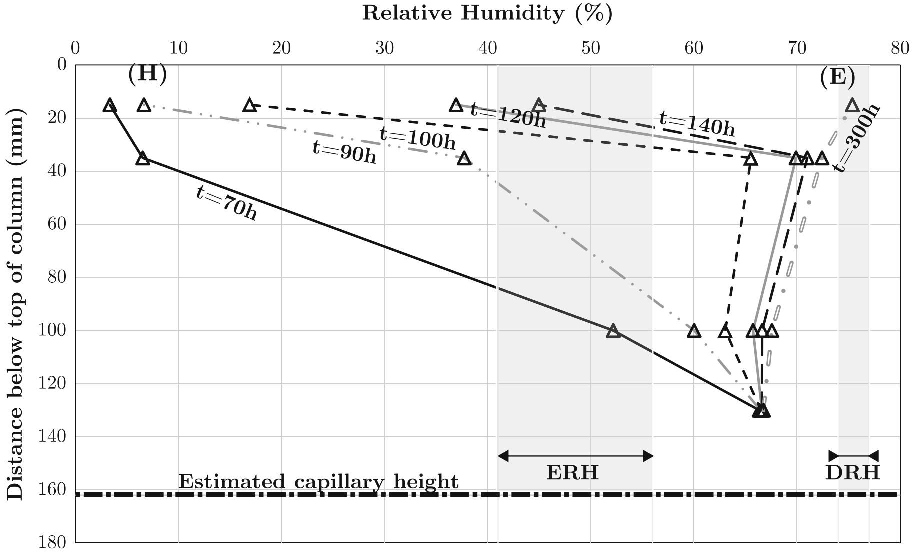

Fig. 10 Relative humidity distribution and evolution according to sensor elevation for experiment 2 showing approximate time of heave (H) and efflorescence (E)

occurs prior to the onset of salt heave, though once subflorescence has commenced the relative humidity increase is rapid. This result concurs with similar claims made by Sghaier et al. (2014).

At a sensor depth of 130 mm, closest to the capillary fringe, the relative humidity remains stable at between 67 and 72 %. This suggests that no general rise in solute level takes place, as otherwise the relative humidity would be close to 75 %. In addition, the relative humidity

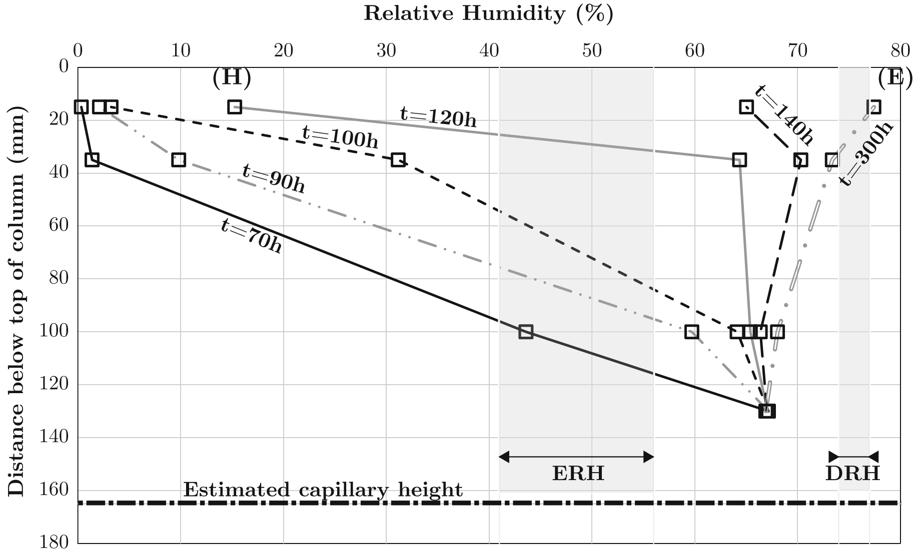

Fig. 11 Relative humidity distribution and evolution according to sensor elevation for experiment 3 showing approximate time of heave (H) and efflorescence (E)

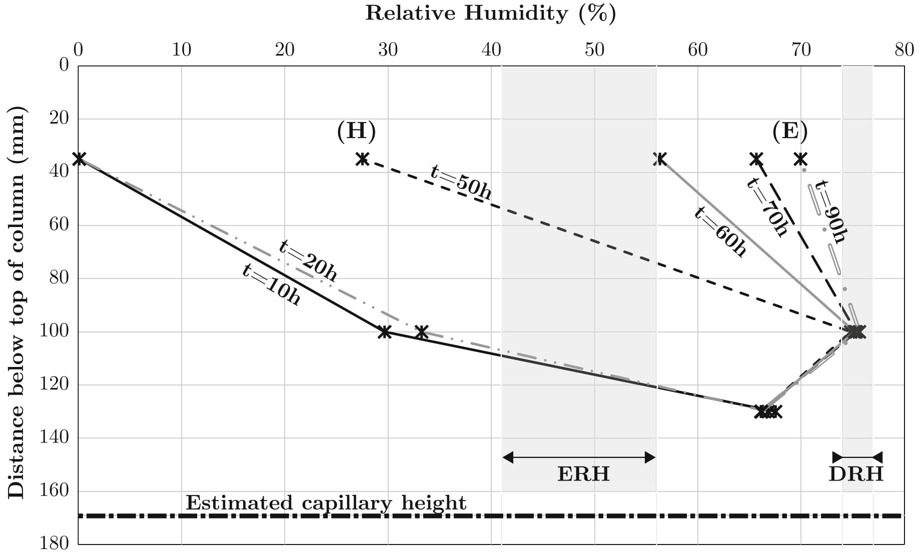

Fig. 12 Relative humidity distribution and evolution according to sensor elevation for experiment 4 showing approximate time of heave (H) and efflorescence (E)

sensor continued to operate normally, suggesting that no solute came in contact with its sensing element. The upward trend in relative humidity towards the top of the sand column is, however, consistent with the extension of occasional dendrites which form at the saturated capillary zone and grow upwards and outwards like the trunk and branches on a tree. Each dendrite would be able to conduct solute upwards by capillary action and release water vapour which can be measured by the RH sensors, but the saturation ratio of the sand between dendrites would remain low.

Compared to the isochronal plot for deionised water, the higher relative humidity close to the sand surface can only suggest the presence of salt dendrites which have overcome the drying effect of the airflow at the top of the column, whereas deionised water could not.

4 Conclusion

Tests with deionised water using TDR probes and relative humidity sensors showed that the initial fluid distribution above the saturated capillary fringe would be insufficient to allow salt diffusion to the top of the column. However, experiments using sensors placed within dry sand in flow columns, aerated at the surface with low humidity air and held at 35 °C, demonstrate upward salt migration from a saturated capillary fringe towards the top of the column. Taken together, these findings show that the brine capillary fringe cannot rise uniformly far enough through dry sand to reach the surface and that observed salt transportation must be through occasional dendrites of salt crystallisation providing additional internal wicks. Measurements of changes in relative humidity coupled with surface displacement show the presence of salt as it migrates beyond the saturated capillary fringe to the surface. Salt is shown to effloresce at the top of the column once the internal salt wicks reach the surface, raising the relative humidity in the neighbouring pores to the point of deliquescence at which crystals and solute can coexist. The experiments have therefore shown that the self-generating wick of salt crystals observed on non-porous surfaces must also occur in porous media, as inferred indirectly through the measurement of water vapour release.

References

Castellazzi, G., Colla, C., de Miranda, S., Formica, G., Gabrielli, E., Molari, L., Ubertini, F.: A coupled multiphase model for hygrothermal analysis of masonry structures and prediction of stress induced by salt crystallisation. Constr. Build. Mater. **41**, 717–731 (2013). doi:10.1016/j.conbuildmat.2012.12.045

Colston, B.J., Watt, D.S., Munro, H.L.: Environmentally induced stone decay: the cumulative effects of crystallisation-hydration cycles on a Lincolnshire oopelsparite limestone. J. Cult. Herit. **4**, 297–307 (2001). doi:10.1016/S1296-2074(01)01129-3

Culligan, P.J., Ivanov, V., Germaine, J.T.: Sorptivity and liquid infiltration into dry soil. Adv. Water Resour. **28**, 1010–1020 (2005). doi:10.1016/j.advwatres.2005.04.003

Desarnaud, J., Derluyn, H., Molari, L., de Miranda, S., Cnudde, V., Shahidzadeh, N.: Drying of salt contaminated porous media: effect of primary and secondary nucleation. J. Appl. Phys. **118**(11), 114901 (2015). doi:10.1063/1.4930292

Desarnaud, J., Shahidzadeh-Bonn, N.: Salt crystal purification by deliquescence/crystallisation cycling. EPL. **95**(48002), 1–6 (2011). doi:10.1209/0295-5075/95/48002

Dopfer, D., Palzer, S., Heinrich, S., Fries, L., Antonyuk, S., Haider, C., Salman, A.D.: Adhesion mechanisms between water soluble particles. Powder Technol. **238**, 35–49 (2013). doi:10.1016/j.powtec.2012.06.029

Eloukabi, H., Sghaier, N., Nasrallah, S.B., Prat, M.: Experimental study of the effect of sodium chloride on drying of porous media: the crusty-patchy efflorescence transition. Int. J. Heat Mass Transfer. **56**(1), 80–93 (2013). doi:10.1016/j.ijheatmasstransfer.2012.09.045

Gao, Y., Chen, S.B., Yu, L.E.: Efflorescence relative humidity of airborne sodium chloride particles: a theoretical investigation. Atmos. Environ. **41**(9), 2019–2023 (2007). doi:10.1016/j.atmosenv.2006.12.014

Hazlehurst, T.H., Martin, H.C., Brewer, L.: The creeping of saturated salt solutions. J. Phys. Chem. **40**(4), 439–452 (1935). doi:10.1021/j150373a003

Hird, R., Bolton, M.D.: Migration of sodium chloride in dry porous materials. Proc. R. Soc. London, Ser. A, 2016 471, (2186) (2016). doi:10.1098/rspa.2015.0710

Hird, R., Bolton, M.D.: Upward migration of sodium chloride by crystallisation on non-porous surfaces. Phil. Mag. **94**(1), 78–91 (2014). doi:10.1080/14786435.2013.843794

Langlet, M., Benali, M., Pezron, I., Saleh, K., Guigon, P., Metlas-Komunjer, L.: Caking of sodium chloride. Role of ambient relative humidity in dissolution and recrystallization process. Chem. Eng. Sci. **86**, 78–86 (2013). doi:10.1016/j.ces.2012.05.014

Likos, W. J., Lu, N.: Automated humidity system for measuring total suction characteristics of clay. Geotech. Test. J. 126(2), 1–12 (2003). doi:10.1520/GTJ11321J

Mohamad, A.A., Sasaki, T., Watanabe, K.: Solute transport through unsaturated soil due to evaporation. J. Environ. Eng., Vol. 126, No. 9 (2000). doi:10.1061/(ASCE)0733-9372(2000)126:9(842)

Mullin, J.W.: Crystallisation, 4th edn. Butterworth Heinemann, Oxford (2001)

Norouzi Rad, M., Shokri, N., Keshmiri, A., Withers, P.J.: Effects of grain and pore size on salt precipitation during evaporation from porous media. Transp. Porous Media. **110**(2), 281–294 (2015). doi:10.1007/s11242-015-0515-8

Or, D., Lehmann, P., Shahraeeni, E., Shokri, N.: Advances in soil evaporation physics—a review. Vadose Zone J. **12**(4), 1–16 (2013). doi:10.2136/vzj2012.0163

Ozdemir, O., Karakashev, S.I., Nguyen, A.V., Miller, J.D.: Adsorption and surface tension analysis of concentrated alkali halide brine solutions. Miner. Eng. **22**(3), 263–271 (2009). doi:10.1016/j.mineng.2008.08.001

Robert, D., Soga, K.: Soil-pipeline interaction in unsaturated soils. In: Laloui, L. (ed.) Mechanics of Unsaturated Geomaterials, pp. 303–325. Wiley, Hoboken (2010)

Robinson, D.A., Jones, S.B., Wraith, J.M., Or, D., Friedman, S.P.: A review of advances in dielectric and electrical conductivity measurement in soils using time domain reflectometry. Vadose Zone J. **2**, 444–475 (2003). doi:10.2136/vzj2003.4440

Rodriguez-Navarro, C., Doehne, E.: Salt weathering: influence of evaporation rate, supersaturation and crystallization pattern. Earth Surf. Proc. Land. **24**, 191–209 (1999). doi:10.1002/(SICI)1096-9837(199903)

Sadeghi, M., Taghikhani, V., Ghotbi, C.: Measurement and correlation of surface tension for single aqueous electrolyte solutions. Int. J. Thermophys. **31**, 852–859 (2010). doi:10.1007/s10765-010-0725-9

Sandrolini, F., Franzoni, E.: An operative protocol for reliable measurements of moisture content in porous materials of ancient buildings. Build. Environ. **41**, 1372–1380 (2006)

Sghaier, N., Prat, M., Nasrallah, S.B.: On the influence of sodium chloride concentration on equilibrium contact angle. Chem. Eng. J. **122**, 47–53 (2006). doi:10.1016/j.cej.2006.02.017

Sghaier, N., Geoffroy, S., Prat, M., Eloukabi, H., Ben Nasrallah, S.: Evaporation-driven growth of large crystallized salt structures in a porous medium. Am. Phys. Soc. Phys. Rev. E **90**, 042402 (2014). doi:10.1103/PhysRevE.90.042402

Sghaier, N., Prat, M.: Effect of efflorescence formation on drying kinetics of porous media. Transp. Porous Media **80**(3), 441–451 (2009). doi:10.1007/s11242-009-9373-6

Stokes, M., Charman, J., Epps, R.J., Griffiths, J.S.: Engineering group working party. Soil and rock description and characteristics. In: Walker, M.J. (ed.) Hot Deserts: Engineering, Geology and Geomorphology, pp. 143–157. Geological Society Engineering Special Publications, London (2012)

Tanaka, M., Girard, G., Davis, R., Peuto, A., Bignell, N.: Recommended table for the density of water between 0C and 40C based on recent experimental reports. Metrologia **38**, 301–309 (2001). doi:10.1088/0026-1394/38/4/3

Terzaghi, K., Peck, R.B.: Soil mechanics in engineering practise. Wiley, New York (1964)

Topp, G.C., Davis, J.L., Annan, A.P.: Electromagnetic determination of soil water content: measurement in coaxial transmission lines. Water Resour. Res. **16**(3), 574–582 (1980). doi:10.1029/WR016i003p00574

Van Enckevort, W.J.P., Los, J.H.: On the creeping of saturated salt solutions. Cryst. Growth Des. **13**(5), 1838–1848 (2013). doi:10.1021/cg301429g

Vargaftik, N.B., Volkov, B.N., Voljak, L.D.: International tables of the surface tension of water. J. Phys. Chem. Ref. Data **12**(3), 817–820 (1983). doi:10.1063/1.555688

Vickers, T., Moukwa, M.: Evaluation of test methods and environmental conditions to promote efflorescence formation under laboratory conditions. J. Test. Eval. **24**(2), 80–83 (1996)

Washburn, E.R.: The creeping of solutions. J. Phys. Chem. **31**(8), 1246–1248 (1926). doi:10.1021/j150278a009

Yang, H., Rahardjo, H., Leong, E.-C., Fedlund, D.G.: Factors affecting drying and wetting soil-water characteristic curves of sandy soils. Can. Geotech. J. **41**, 908–920 (2004)